ARTICLES
https://doi.org/10.1038/s41556-017-0020-0

nature cell biology

Corrected: Author correction

Transient Scute activation via a self-stimulatory loop directs enteroendocrine cell pair specification from self-renewing intestinal stem cells

Jun Chen[1,2], Na Xu[2], Chenhui Wang[2], Pin Huang[2], Huanwei Huang[2], Zhen Jin[2], Zhongsheng Yu[3], Tao Cai[2], Renjie Jiao[3,4] and Rongwen Xi[1,2,5*]

The process through which multiple types of cell-lineage-restricted progenitor cells are specified from multipotent stem cells is unclear. Here we show that, in intestinal stem cell lineages in adult *Drosophila*, in which the Delta-Notch-signalling-guided progenitor cell differentiation into enterocytes is the default mode, the specification of enteroendocrine cells (EEs) is initiated by transient Scute activation in a process driven by transcriptional self-stimulation combined with a negative feedback regulation between Scute and Notch targets. Scute activation induces asymmetric intestinal stem cell divisions that generate EE progenitor cells. The mitosis-inducing and fate-inducing activities of Scute guide each EE progenitor cell to divide exactly once prior to its terminal differentiation, yielding a pair of EEs. The transient expression of a fate inducer therefore specifies both type and numbers of committed progenitor cells originating from stem cells, which could represent a general mechanism used for diversifying committed progenitor cells from multipotent stem cells.

Homeostatic renewal of tissues and organs commonly depends on the resident tissue-specific stem cells, which have the ability to self-renew and produce diverse committed progenitor cells that differentiate into multiple cell types. The generation of lineage-restricted progenitor cells can be actively specified by asymmetric cell division, in which cell fate determinants are specifically segregated into one of two stem cell daughter cells[1]. Alternatively, committed progenitor cells can be specified passively; in this case, stem cells differentiate as they physically depart from the niche environment. Examples are *Drosophila* germline stem cells[2,3] and stem cells in the mouse small intestine[4,5]. However, very little is known about the molecular mechanisms by which distinct, lineage-restricted progenitor cells are generated from a common stem cell pool.

Multipotent intestinal stem cells (ISCs) in the *Drosophila* posterior midgut can differentiate into two distinct cell lineages: absorptive enterocytes (ECs), which have been shown to occur from ~90% of ISC divisions, and secretory enteroendocrine cells (EEs), which occur from ~10% of ISC divisions[6–8]. A typical ISC division generates a new ISC and a post-mitotic enteroblast (EB), the lineage-committed progenitor cell. ISCs produce the membrane-bound ligand Delta (Dl), which activates its receptor Notch in EBs. Notch activation results in unidirectional differentiation of EBs into ECs[6–8]. The process of EE specification, however, is much less well understood. Recent studies have suggested that EEs are directly differentiated from ISCs, implying that the decision of EE specification may occur at the stem cell level in ISCs[9,10], but how this occurs remains unclear. A recent study indicates that, in ~90% of cases, EEs are differentiated directly from ISCs in a process that compromises stemness: an ISC divides once, yielding a pair of EEs[10]. This model is in line with the observation that EEs are typically generated in pairs[6], but it implies that EE generation occurs at the expense of continued existence of ISCs. In view of stem cell maintenance, this seems to be a risky developmental strategy.

Previous studies have demonstrated that the transcription factor Prospero (Pros), which is specifically expressed in EEs, acts as an EE-fate-determination factor[9–11]. The expression of Pros is promoted by the acheate-scute complex (AS-C) genes, and the expression of AS-C genes *scute* (*sc*) and *asense* (*ase*) is normally suppressed by the transcriptional repressor Ttk69[11]. Loss of AS-C genes compromises EE generation without affecting EC generation from ISCs[12,13]. Moreover, overexpressing either Sc or Ase induces increased EE generation from ISCs[12]. However, how Sc is regulated to control EE specification is unclear.

Here, we investigated the regulation of Sc during the process of EE generation, and our results allow us to propose a model through which discrete committed progenitor cell types are generated from stem cells.

Results

An EE-regeneration model reveals that ISCs self-renew during generation of EE pairs. To better understand the process of EE specification in ISCs, we set up an EE regeneration assay and examined de novo EE regeneration. Conditionally depleting *sc* in Esg-GAL4^{ts}, upstream activation sequence (UAS)-sc-RNAi flies by shifting flies to restrictive temperature (RT) (29 °C) from pupal stage caused complete EE depletion in the midgut of newly eclosed flies (Fig. 1a and Supplementary Fig. 1), as previously reported[13]. Shifting flies to RT after eclosion also completely disrupted new EE generation, although some EEs produced from the pupal stage remained (Supplementary Fig. 1). Strikingly, three to four days after shifting EE-less flies back to 18 °C, EEs, marked by Pros, appeared concurrently in many regions of the midgut (Fig. 1b). Interestingly, many cells were co-stained with Dl (membrane) and Pros (nucleus),

[1]Graduate School of Peking Union Medical College, Beijing, China. [2]National Institute of Biological Sciences, Beijing, China. [3]Institute of Biophysics, Chinese Academy of Sciences, Beijing, China. [4]Sino-French Hoffmann Institute, Guangzhou Medical University, Guangzhou, China. [5]Institute for Regenerative Medicine, Shanghai East Hospital, School of Life Sciences and Technology, Tongji University, Shanghai, China. *e-mail: xirongwen@nibs.ac.cn

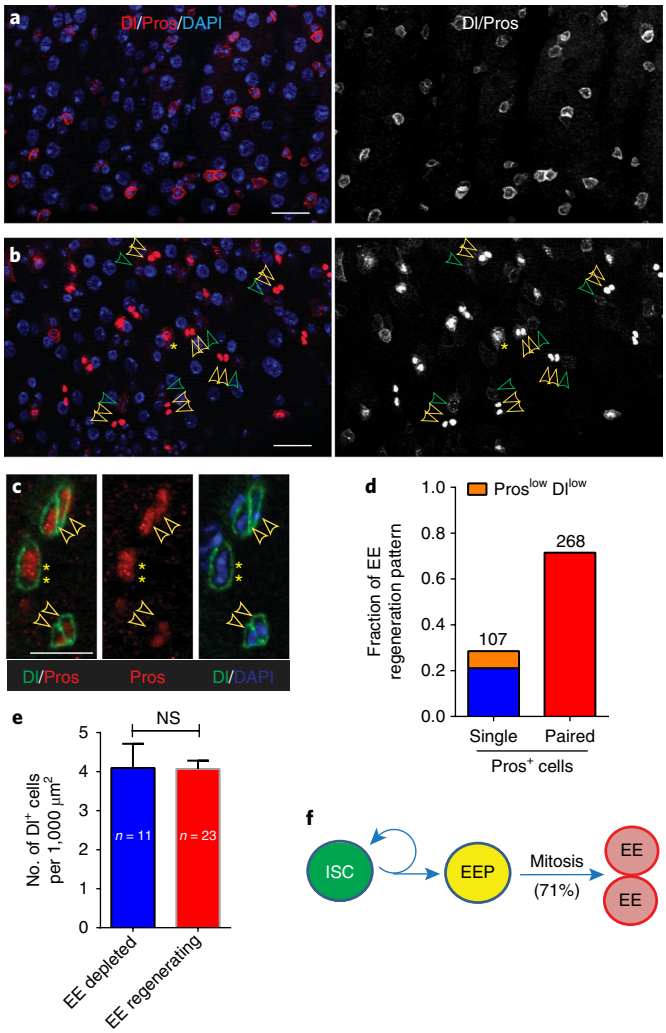

Fig. 1 | An EE-regeneration model reveals that ISCs self-renew during the generation of EE pairs. a–c, Patterns of ISC (marked by anti-Dl, red on membrane) and EE cells (marked by anti-Pros, red in nucleus) during *sc*-RNAi-mediated EE depletion (**a**) and the following EE regeneration (**b**,**c**). Adult midguts of Esg>sc-RNAi shift from the pupal stage were completely deprived of EE cells three days after eclosion. Three-day shift back to 18 °C following EE depletion leads to concurrent EE regeneration. Many intermediate Dl$^+$ Pros$^+$ cells (asterisks) can be detected, and many newly formed EE pairs (yellow arrows) were found adjacent to an ISC (green arrowheads). In **c**, Dl (green) and Pros (red) are stained separately during the EE regeneration process. This experiment was repeated independently three times, with similar results. **d**, Proportion of EE regeneration occurring singly (left column) and in pairs (right column). The single EE column includes Pros^{low} Dl^{low} cells (orange). **e**, Numbers of Dl$^+$ cells per 1,000 µm^2 during EE depletion and EE regeneration. *n*, numbers of flies, as indicated. Significance was measured with unpaired two-tailed *t*-tests. Error bars represent s.e.m. NS, not significant. **f**, Model for the EE regeneration process. An ISC undergoes self-renewal before generating an EEP; 71% of EEPs undergo one round of mitosis to generate a pair of EEs; the rest directly differentiate into a single EE. Scale bars, 20 µm.

and this was further confirmed by separate fluorescent labelling for Dl and Pros (Fig. 1b,c). These Dl$^+$ Pros$^+$ cells are probably the differentiating EEs described previously in normal midgut[9,10]. Similar to what has been observed in normal midgut[6], ~71% of Pros$^+$ cells appeared in pairs (Fig. 1d). The EE pair is probably generated by cell division of a mother cell, as two EEs in the pair appeared simultaneously and mitotic Pros$^+$ cells could be observed (Fig. 1c). After carefully counting the total number of Dl$^+$ cells in the epithelium before and after EE appearance, we found that the number of Dl$^+$ cells remained constant, although Dl expression was downregulated during EE appearance (Fig. 1b,e). In addition, there was always a Dl$^+$ or Dl^{low} cell next to each newly formed EE or EE pair (Fig. 1b). These observations suggest that, instead of directly differentiating into an EE as proposed previously[10], an ISC actually divides first to generate a new EE progenitor cell (EEP), which then undergoes one round of cell division before its terminal differentiation, yielding an EE pair (Fig. 1f). Interestingly, like in normal midgut[6,14], the two EEs in the newly generated EE pair produce different peptide hormones (Supplementary Fig. 2). The EEP is reminiscent of the EE mother cell in the pupal midgut, which is also capable of cell division prior to terminal differentiation[15].

Sc is dynamically expressed in ISCs. Among *AS-C* complex genes, *sc* is both necessary and sufficient for EE specification[12,13]. It is therefore important to understand how *sc* expression is regulated. Using the CRISPR-Cas9 technique, we generated a Sc-GFP knock-in line in which green fluorescent protein (GFP) was fused to 3′ of the Sc coding region (Fig. 2a). The expression pattern of Sc-GFP in larval imaginal discs was virtually identical to the reported *sc* mRNA and protein expression patterns (Supplementary Fig. 3)[16]. In adult midgut, albeit variable in numbers among different midguts, Sc-GFP (GFP fluorescence)-expressing cells were observed only in a subset of Dl$^+$ cells (Fig. 2b,c). By quantification, on average, ~15% of Dl$^+$ cells had distinguishable Sc-GFP expression in both posterior (15.6 ± 2.0% $n = 32$ guts) and anterior (15.5 ± 5.9%, $n = 12$ guts) midguts. Immunostaining with anti-GFP, which greatly amplified the Sc-GFP signal, revealed that Sc-GFP could be observed in virtually all Dl$^+$ cells (Supplementary Fig. 3). Therefore, Sc is dynamically expressed in ISCs, with a weak expression level in most ISCs, and increased expression levels in a small subset of ISCs.

Transient Sc activation induces EE generation from ISCs. From 23 (upstream and downstream) glass multiple reporter (GMR) enhancer-GAL4 lines generated for *sc* (ref. [17]) (Fig. 2d), we identified one line, GMR14C12, that drove UAS-GFP expression in some diploid cells in the midgut epithelium (Fig. 2e,f). The density, distribution and individual variability of the GFP$^+$ cells were largely similar to those of Sc-GFP$^+$ cells, suggesting that this reporter line is driven by the enhancer element for *sc* expression in the midgut. Co-staining with cell markers revealed that GMR14C12>GFP was mainly expressed in 15 ± 0.69% Dl$^+$ cells ($n = 26$ guts), but residual GFP was also often present in the newly formed EEs in the same cell nest (Fig. 2f,g). Interestingly, the GFP$^+$ Dl$^+$ cells commonly showed relatively low levels of Dl expression compared to the GFP$^-$ Dl$^+$ cells (Fig. 2e,f,h). Interestingly, ISCs that are producing EEs are known to be associated with low levels of Dl expression[6]. We also compared the expression pattern between Sc-GFP and GMR14C12-GAL4, UAS-RFP (red fluorescent protein) (GMR14C12>RFP). Similarly, GMR14C12>RFP$^+$ cells were found in small cell nests of two to three cells. About half of them contain Sc-GFP$^+$ cells (Supplementary Fig. 4), suggesting that the GMR14C12->RFP reporter only partially recapitulates Sc-GFP expression in ISCs. This is probably because Sc is expressed transiently and the expression of GMR14C12->RFP is relatively delayed due to the binary expression system used and/or extra time required for RFP maturation. Similar to the GMR14C12>GFP cell nest, many GMR14C12->RFP cell nests also contained newly formed EEs (Supplementary Fig. 4). The residual GMR14C12->RFP or GMR14C12->GFP expression found only in the newly formed EEs but rarely in any ECs indicates that the ISCs with GMR14C12-GAL4 expression only generate EEs. To test this hypothesis, we performed cell lineage tracing studies (Fig. 2i) with flies carrying *GMR14C12-GAL4, Tub-Gal80^{ts}*;

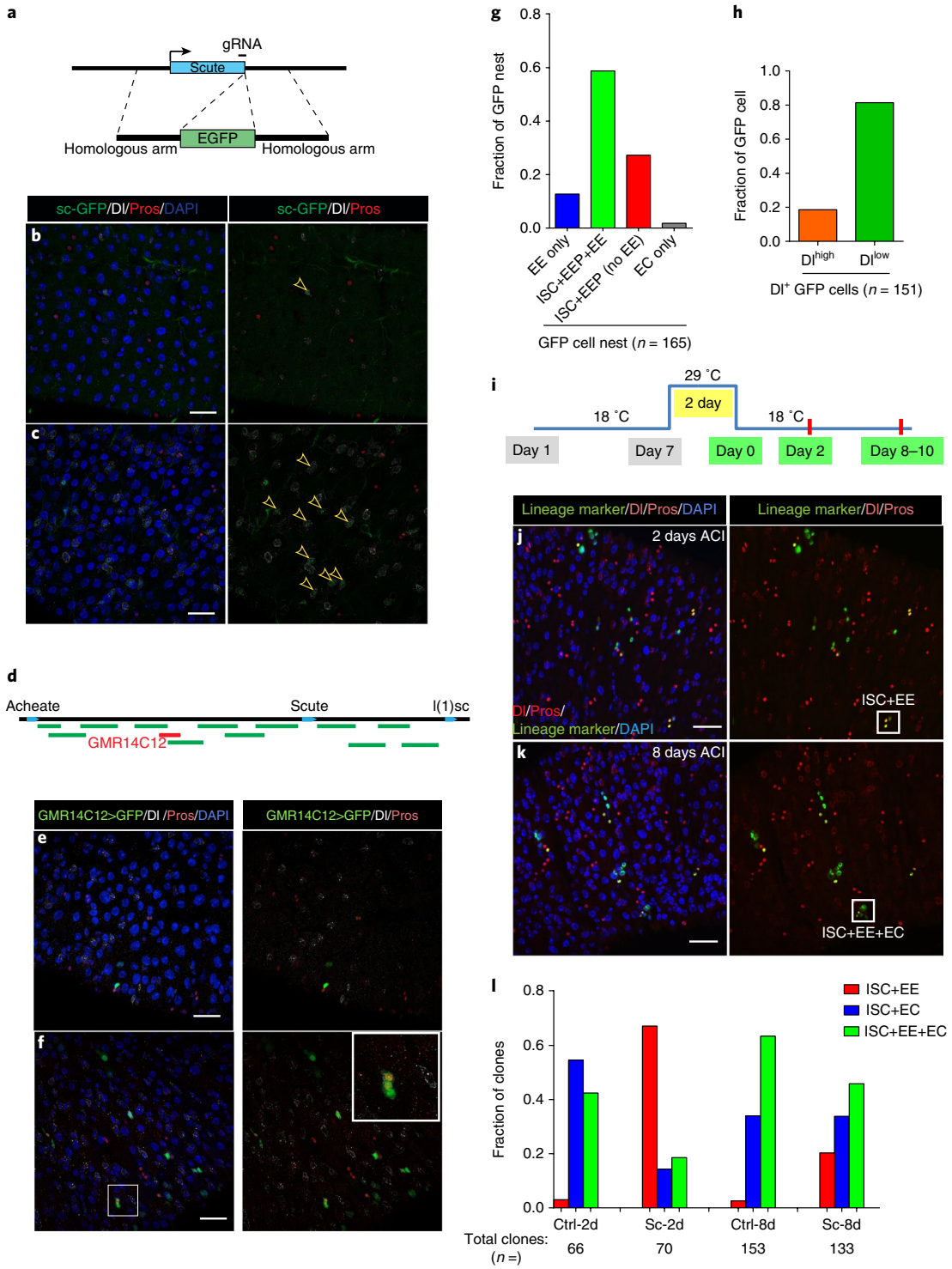

Fig. 2 | Transient Sc expression precedes EE generation from ISCs. a, Diagram showing genomic information for C-terminal insertion of enhanced green fluorescent protein (EGFP) into the *sc* gene region. **b**,**c**, Expression of Sc-GFP (green), Dl (white) and Pros (red) in midgut of five- to seven-day-old flies. Note that in each microscopic field of view, the number of GFP$^+$ cells (arrowheads) could vary significantly from a few (**b**) to a dozen (**c**) cells, possibly reflective of the local proliferation rate. **d**, Diagram showing the genomic regions of GMR-GAL4 lines screened for *sc* midgut enhancer. **e**,**f**, Expression of GMR14C12>GFP (green), Dl (red on membrane) and Pros (red in nucleus) in midgut of five- to seven-day-old flies. The number of GFP$^+$ cell nests varies significantly in different fields of view. GFP was also present in newly formed EEs in the same cell nest (inset). **g**, Classification of GMR14C12>GFP$^+$ cell clusters: EE only (blue column), ISC/EEP+EE (green), ISC/EEP cluster without EE (red) and EC only (grey). **h**, Quantitative analysis of Dl^{high} (red) and Dl^{low} (green) cells within GMR14C12>GFP$^+$ cell clusters. **i**, Diagram showing the strategy for the short- and long-term tracing for GMR14C12-GAL4. **j**,**k**, Expression of lineage marker (green), Dl (red on membrane) and Pros (red in nucleus) in the midgut of GMR14C12-GAL4 flies tracing for 2 days (**j**) and 8 days (**k**). **l**, Classification of marked clones in lineage tracing analysis: ISC+EE (red), ISC+EC (blue) and ISC clone containing both EE and EC (green). In **g**,**h**,**l**, *n* indicates GFP cell nests, Dl$^+$ GFP cells and clones, respectively, as indicated. Samples in **g** and **h** were pooled from 32 animals, and samples in **l** were pooled from four experiments. Experiments were repeated three to five times independently, with similar results. Scale bars, 30 μm.

UAS-flp, Tub-Gal80^{ts}; and the flp-out cassette (*Act<stop<lacZ*)[18]. This analysis revealed that the immediate daughter cells (at day 2 after labelling) of GMR14C12>GAL4$^+$ ISCs were mainly EEs. However, EC daughter cells appeared at 7 days after labelling (Fig. 2j–l), suggesting that transient Sc upregulation in ISCs primes them to generate EEs, and ISCs resume EC production once Sc expression is downregulated.

***Notch* mutant ISCs have increased Sc expression and only give rise to EEs.** It has been shown that loss of *Notch* (*N*) in ISCs causes the formation of Dl$^+$ and Pros$^+$ cell tumours[7,8]. We found that the majority of Dl$^+$ cells in the tumour showed increased expression of Sc-GFP (Fig. 3a). Interestingly, Sc-GFP protein level was transiently downregulated at metaphase of mitosis (Fig. 3a′). In agreement with a recent study[19], the EE-like tumour cells were post-mitotic cells, in contrast to the ISC-like tumour cells (Fig. 3b,c). In addition, BrdU pulse and chase experiments revealed that Dl$^+$ cells could be readily labelled with BrdU, but by chase, the BrdU signal in Dl$^+$ cells quickly disappeared and reappeared in Pros$^+$ cells (Fig. 3d,e), suggesting that the clustered Pros$^+$ cells are derived from Dl$^+$ cells. Consistent with this notion, there are many Dl$^+$ Pros$^+$ cells at the boundary between Dl$^+$ and Pros$^+$ cell clusters (Fig. 3f), and these are probably the cells in the process of EE differentiation. The Dl$^+$ cells in *N* mutant tumour are therefore unipotent: they only give rise to EEs (Fig. 3g). This property of *N* mutant Dl$^+$ cells further supports the notion that increased Sc expression primes ISCs to produce EE progenies.

Sc functions as both a mitogenic factor and a cell-fate inducer. To further understand the function of *sc*, we conditionally induced *sc* expression in ISCs and monitored the cellular events in a time-lapse. Transient *sc* induction caused a rapid cell division response (Fig. 4a,b), revealing that Sc is a potent inducer of cell division. As Sc is known as an EE fate regulator by inducing Pros expression, we examined whether continuous expression of *sc* could cause ISC differentiation into EE. Continuous *sc* expression for a week resulted in dramatic accumulation of Pros$^+$ EEs in the epithelium (Fig. 4c and Supplementary Fig. 5). Cell lineage tracing studies confirmed that *sc*-overexpressing ISCs only generate EEs (Supplementary Fig. 5). After continuous *sc* overexpression in ISCs for 3 weeks, we began to observe regional ISC loss at the anterior midgut (Fig. 4d). Some residual Esg>GFP$^+$ cells co-expressed Pros, indicating that the ISC loss is due to differentiation into EEs. Therefore, although short-time expression of *sc* is not, prolonged activation of *sc* is detrimental to ISC self-renewal/maintenance.

Pros is also known as a potent cell cycle inhibitor[20,21]. Indeed, in contrast to the effect of Sc, conditionally inducing Pros expression immediately caused ISCs to exit the cell cycle (Fig. 4b). Sc is thus both a mitogenic factor and an EE-cell-fate inducer, whereas Pros is both a cell cycle inhibitor and an EE-cell-fate determination factor. These properties underline a precisely regulated circuitry that directs formation of a pair of EEs from each EEP, which will be described below.

Process of *sc*-overexpression-induced EE specification in ISCs. To understand how EEs are generated from ISCs, we examined the cellular events in a time window (24–72 h post *sc* induction) when new EEs just begin to be generated. To do this, we expressed a UAS-RedStinger reporter in the overexpression system. RedStinger is relatively stable and can serve as a lineage marker to trace the progeny of the originally marked ISCs. The number of cell divisions of the initially labelled ISCs could be deduced based on the total number of cells present within each clone. The first cell division following *sc* overexpression occurred in ISCs (PH3$^+$ in a one-cell clone, Fig. 5a), and during mitosis, Pros expression was marginally detectable on the ISC membrane (Fig. 5a). Differential Pros expression

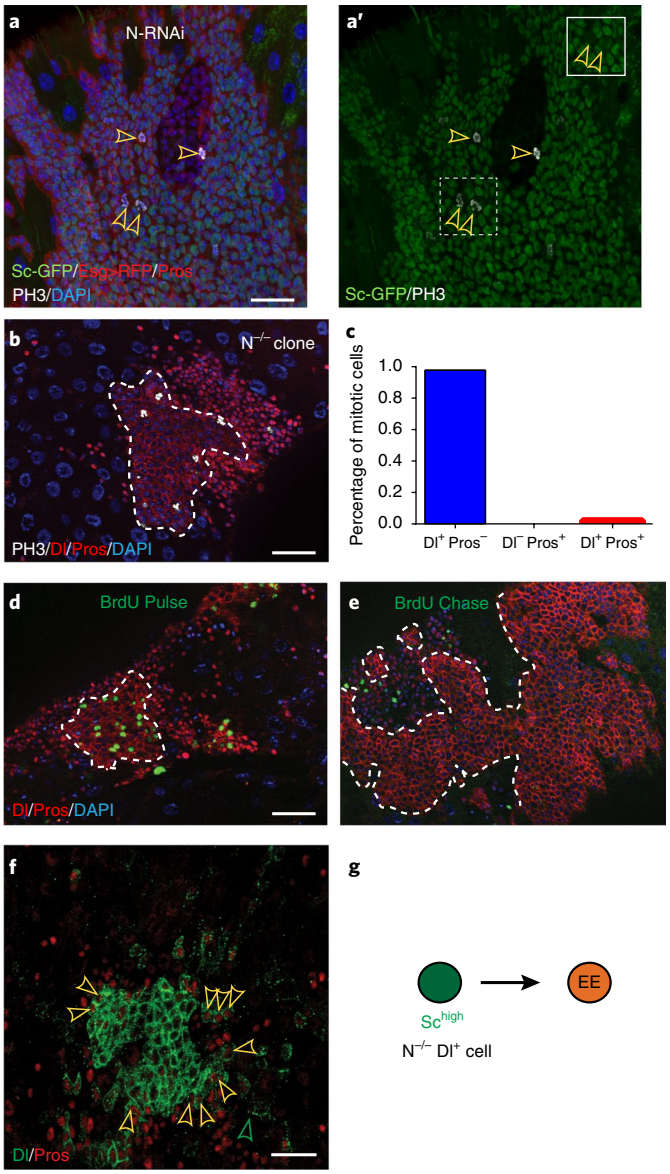

Fig. 3 | Notch mutant ISCs have increased Sc expression and only generate EE cells. a,**a**′, Expression of GFP (green), RFP (red), Pros(red) and PH3 (white) in esg>N-RNAi-induced gut tumor. Arrowhead indicates the PH3$^+$ cells. **b**, Expression of Dl (red on membrane), Pros (red in nucleus) and PH3 (white) in N$^{-/-}$ clone. **c**, Proportion of 3 types of mitotic cells: Dl$^+$ Pros$^-$ (blue column), Dl$^-$ Pros$^-$, and Dl$^+$ Pros$^+$ (red column). A total of 91 PH3$^+$ cells were analyzed, among which 2 cells are Dl$^+$ Pros$^+$, the others are all Dl$^+$ Pros$^-$ cells. **d**,**e**, Expression of Dl (red on membrane), Pros (red in nucleus) and BrdU (green) in N$^{-/-}$ clone of pulse **d** and long-term **e** BrdU incorporation. **f**, Separate staining of Dl (green) and Pros (red) in N$^{-/-}$ clone. Many Dl$^+$ Pros$^+$ cells (indicated by yellow arrowhead) can be detected at the boundary of N$^{-/-}$ tumors. **g**, A diagram showing that N$^{-/-}$ ISC displayed high level of Sc and is primed to differentiate into EE lineage. The experiments in this figure were repeated 3–5 times independently with similar results. Scale bars, 20 μm.

was first observed in cells at telophase, where only one of the two daughter cells retained membrane and cytoplasmic Pros expression (Fig. 5b,f), indicating that the cell division is asymmetric. By contrast, Dl was still evenly expressed in the two daughter cells (Fig. 5f). The Dl$^+$ Pros^{weak} daughter is probably the EEP, which seems to enter mitosis rapidly, as the second cell division (one PH3$^+$ cell in a

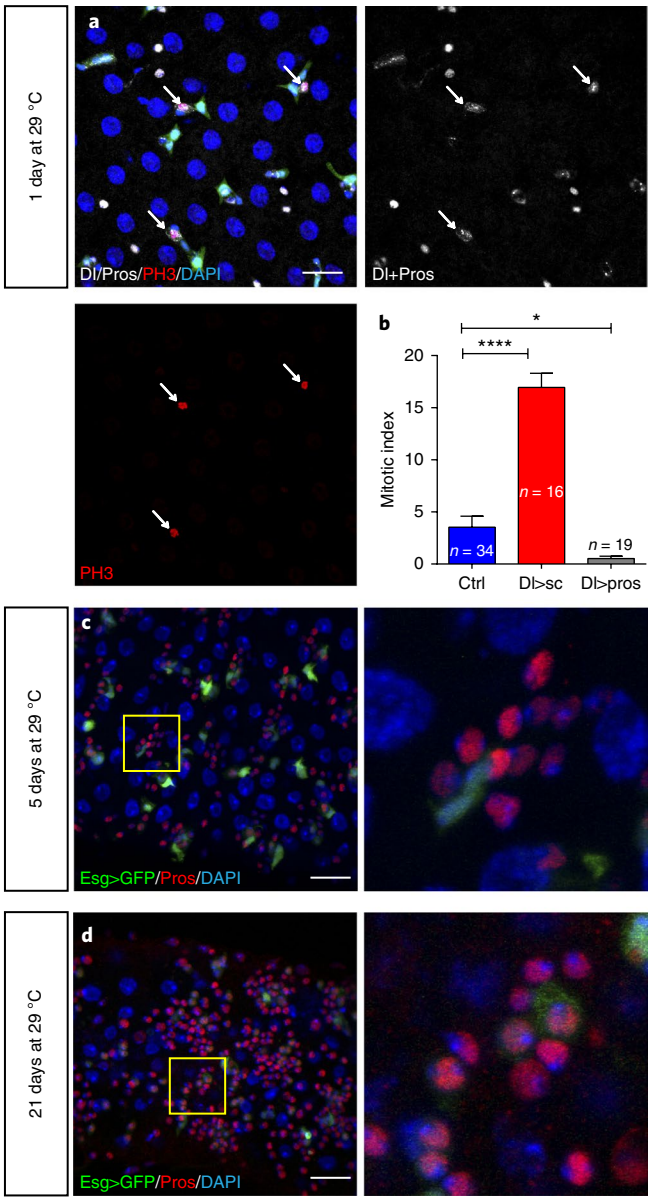

Fig. 4 | Sc functions as both a mitogenic factor and a cell-fate inducer. **a**,**b**, One day of *sc* overexpression led to increased cell proliferation: expression of Esg>GFP (green), Dl (white on membrane), Pros (white in nucleus) and PH3 (red, indicated by white arrow) in the midgut of one-day *sc*-overexpressing flies (**a**); quantification of mitotic cells in wild-type (WT; blue), one-day *sc* overexpression (red) and one-day *pros* overexpression (grey) (**b**). One-day *sc* overexpression greatly increased mitotic cells while one-day *pros* overexpression significantly decreased mitotic cell. *n* represents number of midgets, as indicated. Significance was measured with unpaired two-tailed *t*-tests. Error bars represent s.e.m. $^{****}P < 0.0001$; $^{*}P < 0.05$ ($P = 0.0408$). **c**,**d**, Expression of Esg>GFP (green), Dl (white) and Pros (red) in midguts of 5-day (**c**) and 21-day (**d**) *sc*-overexpressing flies. In **c**, short-term overexpression of *sc* induces continuous EE lineage differentiation without disrupting ISC maintenance. In **d**, long-term induction of *sc* leads to ISC loss in the anterior gut. Note that many GFP$^+$ cells have Pros expressed (enlarged insets), indicative of precocious EE differentiation. Experiments were repeated three to five times independently, with similar results. Scale bars, 20 μm.

two-cell clone, Fig. 5c) following *sc* overexpression always happened in these cells, before the original ISC re-enters mitosis (in a three-cell clone, Fig. 5e). During mitosis, EEPs began to have strong and punctate nuclear Pros expression (Fig. 5c,d,g), indicative of the initiation of EE commitment.

Collectively, these observations suggest a stepwise model for EE regeneration from ISCs: transient activation of *sc* expression induces asymmetric cell division, which generates a new ISC and an EEP. Sc also induces Pros expression, but the nuclear translocation and transcriptional activity of Pros can only occur in EEPs, not ISCs. Residual Sc activity in the newly formed EEP then induces one round of cell division before the accumulation of nuclear Pros that causes the cell cycle exit and EE commitment. In this manner, precisely a pair of EEs is generated from each EEP (Fig. 5h).

Two regulatory feedback loops control transient Sc activation in ISCs. It is intriguing how this transient activation of Sc is achieved. A feedback mechanism via Slit-Robo2 signalling has been implicated in regulating EE generation[9,22], but we found that the Slit-Robo2 signalling does not affect Sc expression in ISCs (Supplementary Fig. 3). Previous studies on early *Drosophila* development have suggested reciprocal regulatory relationships between *AS-C* genes and the enhancer of split complex (*E(spl)*) genes, which are known as the Notch target genes[23–27]. To test whether similar mechanisms occur in ISCs, we screened a number of lacZ, GAL4 or GFP reporters or candidate reporters for individual *E(spl)* genes[28]. m3>GFP and mβ-lacZ showed patterns similar to the general Notch activation reporter NRE-lacZ, which is specifically expressed in EBs. Interestingly, m8-lacZ showed a very weak, but similar expression pattern to Sc (Fig. 6a–c): it was weakly detectable in a small subset of diploid cells. Moreover, m8-lacZ$^+$ cells were largely overlapped with GMR14C12>GFP$^+$ cells (Fig. 6a,b). In addition, the majority of E(spl)m8-lacZ$^+$ ISCs were Dl^{low} (Fig. 6b), again similar to the profile of GMR14C12>GFP$^+$ cells (Fig. 2h). This indicates a direct regulatory relationship between Sc and E(spl)m8. Indeed, transient overexpression of *sc* in ISCs led to robust upregulation of m8-lacZ expression in all progenitor cells (Fig. 6c–e). In addition, ectopic expression of *sc* in ECs using MyoIA-GAL4 also led to ectopic m8-lacZ expression in ECs (Fig. 6f). Notably, co-expressing Notch-RNAi did not prevent the upregulation of m8-lacZ expression caused by *sc* overexpression (Fig. 6g,h), suggesting that *E(spl)m8* expression is independent of Notch activity in ISCs.

To further characterize the regulatory relationship between *sc* and *E(spl)* genes, we transiently overexpressed *sc* in ISCs by Dl-GAL4 and sorted out Dl>GFP$^+$ cells for RNA-seq analysis. From this analysis, we found that, in addition to *m8*, many other *E(spl)* genes, such as *m4*, *m6*, *m7*, *mγ* and *mδ*, were significantly upregulated as well (>100-fold) upon *sc* overexpression (Fig. 6i). The analysis also revealed that *sc* overexpression strongly induced the expression of multiple cell cycle-promoting genes, such as *stg*, *CycA*, *CycB* and *CycE* (Fig. 6i), further supporting that Sc is a potent mitogenic factor. By analysing previously reported ChIP-seq data for Sc in ISCs[29], we found that Sc could bind to the enhancer regions of multiple *E(spl)* genes, including *mγ*, *m6*, *m7* and *m8* (Supplementary Fig. 6), suggesting that Sc directly regulates their transcription. In the enhancer sequence for *m8*, we identified two consensus E-box sites (CANNTG) for proneural factors, named here E-box #1 (E1) and E-box #2(E2) (Supplementary Fig. 6). Mutation of E1 severely dampened lacZ reporter expression in response to *sc* induction, while mutation of E2 only mildly (if at all) reduced the reporter expression (Supplementary Fig. 6), suggesting that the E1 site is a major Sc-binding site in the *E(spl)m8* enhancer.

To study the effect of *E(spl)* genes on *sc*, we found that transient overexpression of *E(spl)m8* rapidly eliminated sc-GFP expression in all ISCs (Fig. 7a,b), and also rapidly suppressed Dl expression in ISCs (Fig. 7a,b). This explains the decreased Dl expression in ISCs during EE regeneration as well as in GMR14C12>GFP$^+$ cells and m8-lacZ$^+$ cells. To determine whether or not *E(spl)m8* suppresses *sc* expression directly, we expressed *E(spl)m8-Dam* fusion gene in

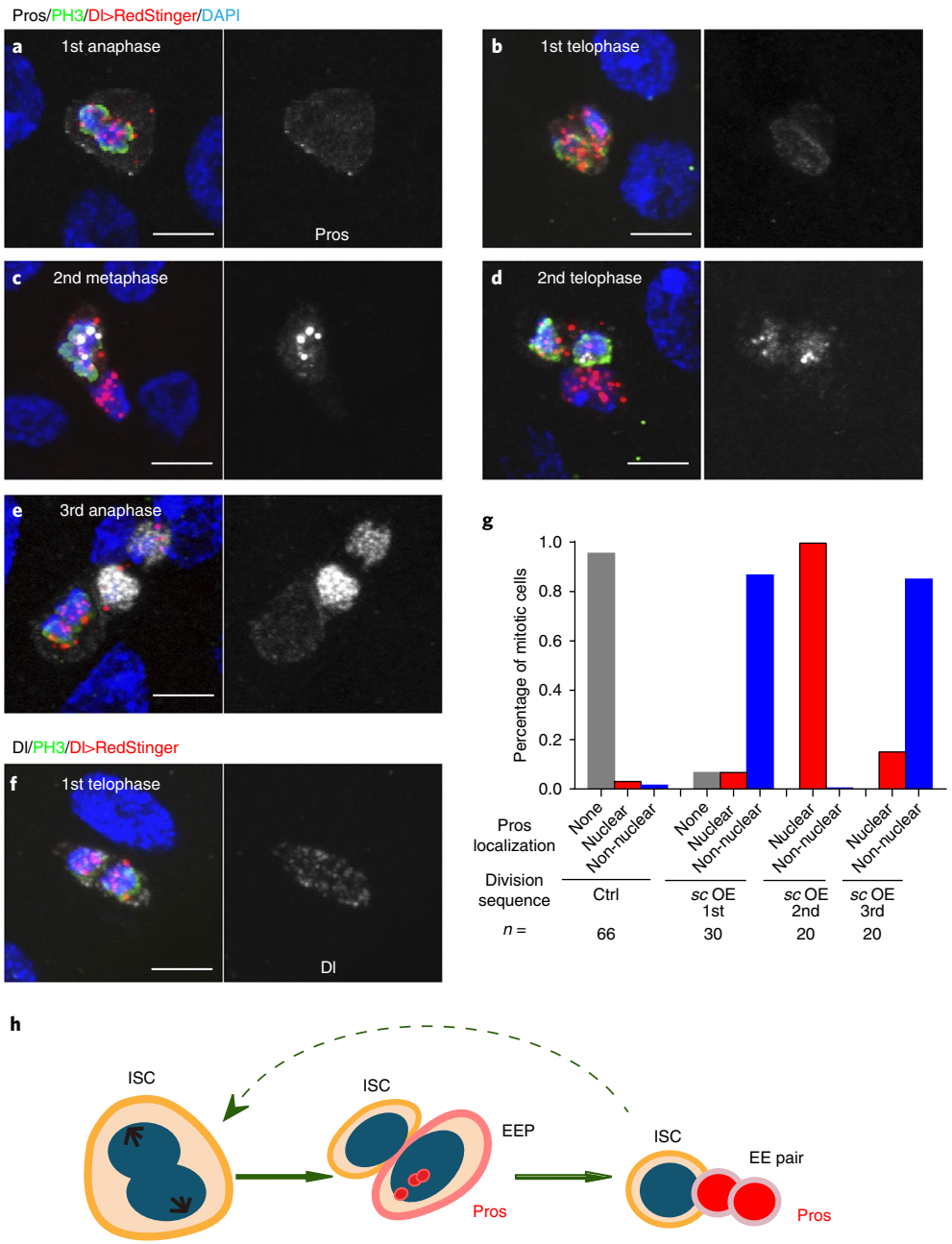

Fig. 5 | Process of *sc*-overexpression-induced EE generation from ISCs. a–e, Expression of Dl>RedStinger (red), PH3 (green) and Pros (white) during *sc*-overexpression-induced mitosis. The order of cell division can be deduced based on the mitotic marker PH3 and the number of RedStinger cells in a single cluster. **a**, Pros showed marginal expression on membrane at anaphase of the first cell division, which occurs in ISCs. **b**, At telophase of the first cell division, one of the two daughter cells began to show cytoplasmic Pros accumulation. **c**,**d**, The second cell division always occurred in the Pros$^+$ daughter cell. During mitosis, Pros began to accumulate in the nucleus with a punctate pattern. **e**, The third cell division occurred again in ISCs. **f**, Expression of Dl>RedStinger (red), PH3 (green) and Dl (white) in ISCs during *sc*-overexpression-induced mitosis. Dl did not show differential level during asymmetric cell division. **g**, Quantitative analysis of Pros subcellular localization in mitotic cells during the first (ISC), second (EEP) and third (ISC) cell divisions: no detectable expression (grey), nuclear expression (red) and membrane expression (blue). *n* represents RedStinger clones, as indicated. **h**, Graphic model for the process of EE generation from ISCs with continuous *sc* expression. *sc* induction in ISCs promotes asymmetric cell division that generates EEPs, which begin to show punctate nuclear Pros expression. Each EEP immediately divides once before terminal differentiation, yielding a pair of EEs. Experiments were repeated three to five times independently, with similar results. Scale bars, 5 µm.

ISCs, and performed DNA adenine methyltransferase identification (DamID) analysis. Interestingly, we observed a strong and specific enrichment peak at the GMR14C12 region (Fig. 7e), suggesting that E(spl)m8 is able to directly bind to the enhancer of *sc* in ISCs. The direct two-way regulation between Sc and E(spl)m8 further supports the notion that Sc and E(spl)m8 (plus other E(spl) proteins) form a negative feedback regulatory loop in ISCs, which may explain the transient activation pattern of Sc in ISCs.

To test the functional requirement of *E(spl)* genes in suppressing *sc* expression, we generated MARCM clones mutant for *Df(3R) E(spl) b32.2 gro+*, a deletion and transgene combination in which all of the *E(spl)* genes have been removed[30]. Consistent with previous

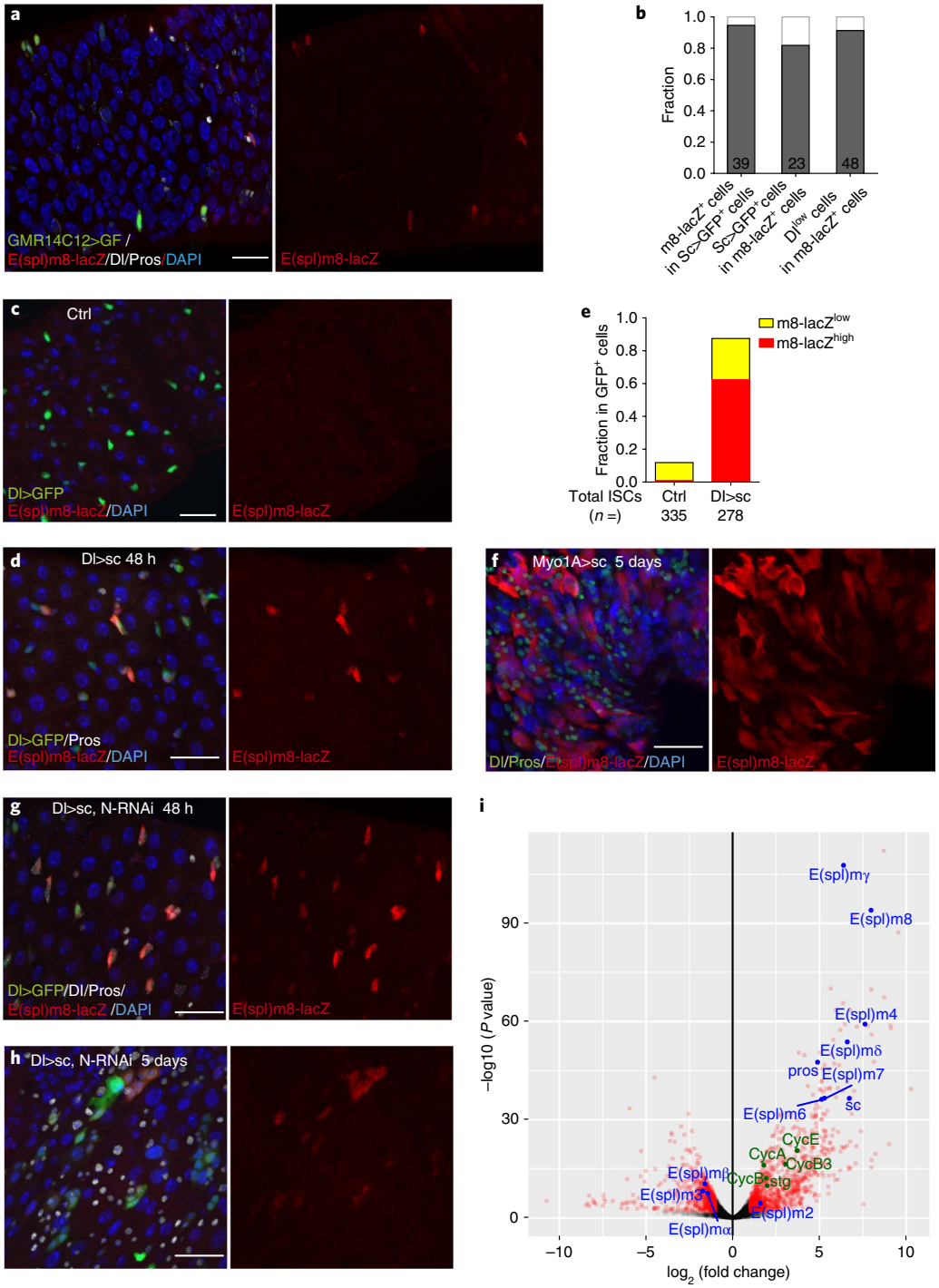

Fig. 6 | Sc induces E(spl) genes in ISCs. a, Expression of GMR14C12>GFP (green), E(spl)m8-lacZ (red) and Pros (white) in midgut of adult flies. **b**, Quantitative analysis of cell proportion of E(spl)m8-lacZ/GMR14C12>GFP^{+} (left), GMR14C12>GFP^{+}/ E(spl)m8-lacZ^{+} (middle), Dl^{low}/ E(spl)m8-lacZ^{+} cells (right). *n* represents total cells (pooled from 24 animals), as indicated. **c**,**d**, Expression of Dl>GFP (green), E(spl)m8-lacZ (red), Dl (white on membrane) and Pros (white in nuclear) in ctrl (**c**) and *sc*-overexpressing midguts (**d**). Overexpression of *sc* in ISCs led to robust upregulation of m8-lacZ expression in all progenitor cells. Note that for the lacZ staining images in **c** and **d**, the same exposure time was used for comparison. **e**, Quantitative analysis of cell proportion of E(spl)m8-lacZ^{+} cells in ctrl (left) and *sc*-overexpressing midgut (right). The population of E(spl)m8-lacZ^{+} cells was classified into two types: E(spl)m8 ^{high} (red) and E(spl)m8 ^{low} (yellow). *n* represents ISCs (pooled from 25 animals), as indicated. **f**, Expression of E(spl)m8-lacZ (red), Dl (green on membrane) and Pros (green in nuclear) with *sc* overexpression in ECs by Myo1A-GAL4. Ectopic expression of m8-lacZ expression was found in ECs. **g**,**h**, Expression of Dl>GFP (green), E(spl)m8-lacZ (red), Dl (white on membrane) and Pros (white in nucleus) with co-expression of *sc* and *Notch-RNAi* for two days (**g**) and five days (**h**). Co-expressing *Notch-RNAi* did not prevent the upregulation of m8-lacZ expression caused by *sc* overexpression. Note that *sc* overexpression prevented N-RNAi-induced tumour development by promoting EE differentiation. **i**, Scatter plot showing the comparison of gene expression profiles of Dl>GFP^{+} cells in WT and *sc*-overexpressing midgut. Pink dots depict genes with twofold and higher changes, including decreased genes (left) and increased genes (right). Both WT and *sc* overexpression datasets have three biological replicates. Experiments were repeated three to five times independently, with similar results. Scale bars, 20 μm.

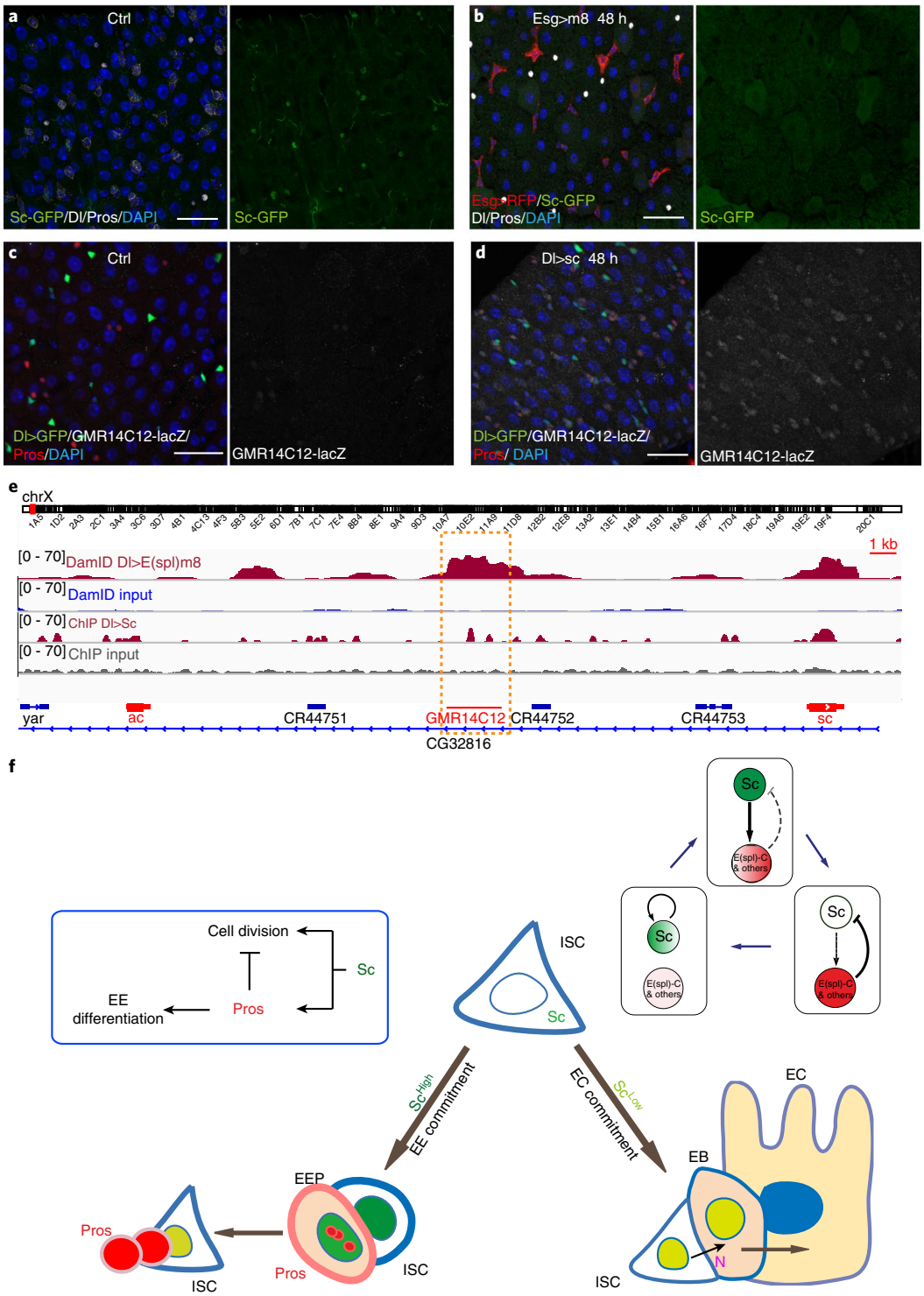

Fig. 7 | Regulatory feedback loops control Sc expression in ISCs. a,**b**, Expression of Esg>RFP (red), Sc-GFP (green), Dl (white on membrane) and Pros (white in nucleus) in midguts of WT (**a**) and *m8*-overexpressing midgut (**b**). Overexpression of *m8* rapidly reduced sc-GFP and Dl expression in all ISCs (**b**). **c**,**d**, Expression of Dl>GFP (green), GMR14C12-lacZ (white) and Pros (red) in the midgut of WT (**c**) and *sc*-overexpressed midgut (**d**). GMR14C12-lacZ was nearly undetectable in normal midgut epithelium. Overexpression of *sc* in ISCs led to GMR14C12-lacZ expression in progenitor cells and newly formed EEs. Experiments were repeated three to five times independently, with similar results. **e**, DamID analysis for E(spl)m8 and ChIP-seq analysis for Sc in ISCs revealed binding activities for both E(spl)m8 and Sc at the GMR14C12 region. **f**, Graphic model to describe how ECs and EEs are respectively generated from ISCs. In the ISC lineages of adult *Drosophila* midgut, Delta-Notch-signalling-guided EC generation from ISCs acts as the default mode, while transient expression of Sc triggers EE generation from ISCs. Oscillatory expression of Sc in ISCs is achieved by transcriptional self-stimulation combined with negative feedback regulation between Sc and E(spl) proteins and other Notch targets. During generation of EEs, increased Sc expression induces asymmetric cell division that generates a new ISC and an EEP. Because Sc functions both as a mitogenic factor and a cell-fate inducer, residual Sc activity in the newly formed EEP is then able to induce one round of cell division before accumulation of nuclear Pros causes the cell cycle exit and EE differentiation. In this manner, precisely a pair of EEs is generated from each EEP. Scale bars, 30 μm (**a**,**b**,**d**), 20 μm (**c**).

observations[12], the mutant clones contained increased number of Dl$^+$ cells, and further properly differentiated ECs, but not EEs (Supplementary Fig. 3). We found that there was no obvious upregulation of sc-GFP expression in any of the ISC-like cells within the *Df(3R) E(spl) b32.2 gro* + mutant clones (25 clones examined, corresponding to 416 Dl$^+$ cells). One likely possibility is that, in addition to the *E(spl)* genes, there are other Notch downstream target genes that function to promote EC differentiation, and that participate in negative feedback regulation with *sc*. Conceivably, the loss of *E(spl)* genes may possibly cause compensatory upregulation of such unidentified genes in a manner that prevents the activation of *AS-C* genes, and that primes all of the undifferentiated cells to adopt an EC fate.

Sc has been reported to transcriptionally self-stimulate itself, which acts as an essential mechanism for proneural protein accumulation during sensory organ development[25,31]. To test whether this also occurs in ISCs, we constructed LacZ reporter for *sc* using the GMR14C12 enhancer fragment. GMR14C12-lacZ was barely detectable in WT midgut epithelium. However, overexpression of *sc* (2 days at RT) by Dl-GAL4 effectively induced lacZ reporter expression in many diploid cells in the epithelium, including ISCs, presumptive EEPs, and newly formed EEs (Fig. 7c,d). The Sc ChIP-seq data analysis also revealed two Sc binding peaks within the GMR14C12 region (Fig. 7e). Together, these data suggest that Sc is able to stimulate its own transcription directly by binding to the *sc* enhancer, and this self-stimulation may allow Sc to gradually accumulate to a relatively high level before being shut down via feedback regulation.

Collectively, these data suggest a model to explain the dynamic Sc expression in ISCs. Sc is usually expressed at low levels, and *E(spl)* genes are not expressed. Through transcriptional self-stimulation, Sc gradually builds up and eventually reaches a level that is sufficient to induce EEP generation. Concomitantly, the high level of Sc also induces *E(spl)* genes. These induced E(spl) proteins and other unidentified Notch targets then function as a negative-feedback mechanism that rapidly turns *sc* expression back to the baseline level. The expression of *E(spl)* genes is consequently downregulated, and the expression of both E(spl) proteins and Sc then returns to the default states (Fig. 7f).

The production of EEs from pupal ISCs (pISCs) occurs at ~48–72 h after pupal formation (APF) (Supplementary Fig. 7)[15,32–35], and we found that transient expression of Sc directs EE generation in pupal ISCs as well.

Discussion

This study suggests a simple model to describe how ECs and EEs are respectively generated from ISCs: Delta-Notch-signalling-guided EC generation from ISCs acts as the default mode, while transient Sc expression triggers EE generation from ISCs (Fig. 7f).

The finding that a cell-fate inducer is expressed in stem cells to induce progenitor cell specification is unexpected, as expression of a cell-fate inducer could potentially compromise stem cell maintenance by promoting differentiation. As we have demonstrated, overexpressing *sc* in ISCs for a prolonged time is able to deplete ISCs by forcing their differentiation. Under normal conditions, however, Sc expression is only transiently increased. In addition, although Sc is sufficient to induce Pros expression in ISCs, Pros protein is only marginally detectable, strictly localized to the cell membrane and/or cytoplasm of ISCs. This indicates that there are additional mechanisms through which Pros activation is prevented in ISCs, such as by destabilizing Pros or preventing Pros from entering the nucleus, mechanisms that are utilized in neural stem cell lineages[36,37]. Therefore, transient expression of a cell-fate inducer is a seemingly risky but rather safeguarded mechanism by which lineage-committed progenitors are generated from stem cells.

Sc is dynamically expressed in ISCs, and our study suggests that this dynamic expression pattern is driven by a coordinated action of two feedback loops: a transcriptionally self-stimulatory loop of Sc and a negative feedback loop between Sc and E(spl) proteins. As the depletion of the entire *E(spl)* genes does not lead to continuous activation of Sc, it is likely that other Notch downstream targets or other mechanisms could also participate in this negative feedback loop. For instance, a Sina-Phyl-Ttk69 complex has recently been implicated in a feedback loop with Sc to regulate EE differentiation[38]. Given that the negative feedback is a common mechanism underlying biochemical oscillations[39], these feedback interplays could provide a mechanism that drives oscillatory expression of Sc in ISCs. This hypothesis is attractive, because Sc oscillation could potentially serve as an internal timer for periodic production of EEs from ISCs. Future cellular and molecular analysis combined with *in vivo* live imaging should help to further test and refine this oscillation model, and to understand whether and how this internal timer is regulated with environmental cues.

Lineage-committed progenitor cells usually transiently amplify themselves prior to terminal differentiation. For instance, the transit-amplifying progenitor cells in mammalian small intestine usually divide four to five times before terminal differentiation[40]. Similarly, each ganglion mother cell in *Drosophila* neuroblasts divides exactly once prior to terminal differentiation, which yields a pair of neurons or glial cells[41], akin to the EE pair generation from an EEP reported here. We find that Sc is both a mitogenic factor and a cell-fate inducer. Pros, on the other hand, is a known inhibitor of cell division and a cell differentiation factor[42]. Because of these properties, the net result of the diminishing and accumulating activity of Sc and Pros, respectively, guides each EEP to divide exactly once prior to terminal differentiation, yielding an EE pair (Fig. 7f). Our study therefore also demonstrates a mechanism that determines the number of transient amplifications of committed progenitor cells.

In summary, our study demonstrates that the transient expression of a fate inducer specifies both the type and the cell division number of committed progenitor cells from multipotent stem cells. Recent studies on progenitor cells in mammalian tissues have found that the expression of fate-inducing transcription factors is frequently detected in self-renewing stem cells[43–45], indicating that this seemingly risky but safely guarded mechanism reported here could represent a general principle for producing several distinct types of committed progenitor cell from the same pool of multipotent stem cells.

Methods

Methods, including statements of data availability and any associated accession codes and references, are available at https://doi.org/10.1038/s41556-017-0020-0.

Received: 10 January 2017; Accepted: 1 December 2017;
Published online: 15 January 2018

References

1. Neumuller, R. A. & Knoblich, J. A. Dividing cellular asymmetry: asymmetric cell division and its implications for stem cells and cancer. *Genes. Dev.* **23**, 2675–2699 (2009).
2. Morrison, S. J. & Spradling, A. C. Stem cells and niches: mechanisms that promote stem cell maintenance throughout life. *Cell* **132**, 598–611 (2008).
3. Li, L. & Xie, T. Stem cell niche: structure and function. *Annu. Rev. Cell. Dev. Biol.* **21**, 605–631 (2005).
4. Snippert, H. J. et al. Intestinal crypt homeostasis results from neutral competition between symmetrically dividing Lgr5 stem cells. *Cell* **143**, 134–144 (2010).
5. Lopez-Garcia, C., Klein, A. M., Simons, B. D. & Winton, D. J. Intestinal stem cell replacement follows a pattern of neutral drift. *Science* **330**, 822–825 (2010).
6. Ohlstein, B. & Spradling, A. Multipotent *Drosophila* intestinal stem cells specify daughter cell fates by differential notch signaling. *Science* **315**, 988–992 (2007).
7. Ohlstein, B. & Spradling, A. The adult *Drosophila* posterior midgut is maintained by pluripotent stem cells. *Nature* **439**, 470–474 (2006).
8. Micchelli, C. A. & Perrimon, N. Evidence that stem cells reside in the adult *Drosophila* midgut epithelium. *Nature* **439**, 475–479 (2006).

9. Biteau, B. & Jasper, H. Slit/Robo signaling regulates cell fate decisions in the intestinal stem cell lineage of *Drosophila*. *Cell. Rep.* **7**, 1867–1875 (2014).
10. Zeng, X. & Hou, S. X. Enteroendocrine cells are generated from stem cells through a distinct progenitor in the adult *Drosophila* posterior midgut. *Development* **142**, 644–653 (2015).
11. Wang, C., Guo, X., Dou, K., Chen, H. & Xi, R. Ttk69 acts as a master repressor of enteroendocrine cell specification in *Drosophila* intestinal stem cell lineages. *Development* **142**, 3321–3331 (2015).
12. Bardin, A. J., Perdigoto, C. N., Southall, T. D., Brand, A. H. & Schweisguth, F. Transcriptional control of stem cell maintenance in the *Drosophila* intestine. *Development* **137**, 705–714 (2010).
13. Amcheslavsky, A. et al. Enteroendocrine cells support intestinal stem-cell-mediated homeostasis in *Drosophila*. *Cell. Rep.* **9**, 32–39 (2014).
14. Beehler-Evans, R. & Micchelli, C. A. Generation of enteroendocrine cell diversity in midgut stem cell lineages. *Development* **142**, 654–664 (2015).
15. Guo, Z. & Ohlstein, B. Stem cell regulation. Bidirectional Notch signaling regulates *Drosophila* intestinal stem cell multipotency. *Science* **350**, aab0988 (2015).
16. Cubas, P., de Celis, J. F., Campuzano, S. & Modolell, J. Proneural clusters of achaete-scute expression and the generation of sensory organs in the *Drosophila* imaginal wing disc. *Genes. Dev.* **5**, 996–1008 (1991).
17. Jenett, A. et al. A GAL4-driver line resource for *Drosophila* neurobiology. *Cell. Rep.* **2**, 991–1001 (2012).
18. Struhl, G. & Basler, K. Organizing activity of wingless protein in *Drosophila*. *Cell* **72**, 527–540 (1993).
19. Patel, P. H., Dutta, D. & Edgar, B. A. Niche appropriation by *Drosophila* intestinal stem cell tumours. *Nat. Cell. Biol.* **17**, 1182–1192 (2015).
20. Lai, S. L. & Doe, C. Q. Transient nuclear Prospero induces neural progenitor quiescence. *eLife* **3**, e03363 (2014).
21. Li, L. & Vaessin, H. Pan-neural Prospero terminates cell proliferation during *Drosophila* neurogenesis. *Genes. Dev.* **14**, 147–151 (2000).
22. Zeng, X. et al. Genome-wide RNAi screen identifies networks involved in intestinal stem cell regulation in *Drosophila*. *Cell. Rep.* **10**, 1226–1238 (2015).
23. Singson, A., Leviten, M. W., Bang, A. G., Hua, X. H. & Posakony, J. W. Direct downstream targets of proneural activators in the imaginal disc include genes involved in lateral inhibitory signaling. *Genes. Dev.* **8**, 2058–2071 (1994).
24. Nellesen, D. T., Lai, E. C. & Posakony, J. W. Discrete enhancer elements mediate selective responsiveness of enhancer of split complex genes to common transcriptional activators. *Dev. Biol.* **213**, 33–53 (1999).
25. Culi, J. & Modolell, J. Proneural gene self-stimulation in neural precursors: an essential mechanism for sense organ development that is regulated by Notch signaling. *Genes. Dev.* **12**, 2036–2047 (1998).
26. Jimenez, G. & Ish-Horowicz, D. A chimeric enhancer-of-split transcriptional activator drives neural development and achaete–scute expression. *Mol. Cell. Biol.* **17**, 4355–4362 (1997).
27. Dawson, S. R., Turner, D. L., Weintraub, H. & Parkhurst, S. M. Specificity for the hairy/enhancer of split basic helix-loop-helix (bHLH) proteins maps outside the bHLH domain and suggests two separable modes of transcriptional repression. *Mol. Cell. Biol.* **15**, 6923–6931 (1995).
28. Housden, B. E., Li, J. & Bray, S. J. Visualizing Notch signaling in vivo in *Drosophila* tissues. *Methods Mol. Biol.* **1187**, 101–113 (2014).
29. Li, Y. et al. Transcription factor antagonism controls enteroendocrine cell specification from intestinal stem cells. *Sci. Rep.* **7**, 988 (2017).
30. Schrons, H., Knust, E. & Campos-Ortega, J. A. The enhancer of split complex and adjacent genes in the 96F region of *Drosophila melanogaster* are required for segregation of neural and epidermal progenitor cells. *Genetics* **132**, 481–503 (1992).
31. Martinez, C., Modolell, J. & Garrell, J. Regulation of the proneural gene achaete by helix-loop-helix proteins. *Mol. Cell. Biol.* **13**, 3514–3521 (1993).
32. Jiang, H. & Edgar, B. A. EGFR signaling regulates the proliferation of *Drosophila* adult midgut progenitors. *Development* **136**, 483–493 (2009).
33. Takashima, S. et al. Development of the *Drosophila* entero-endocrine lineage and its specification by the Notch signaling pathway. *Dev. Biol.* **353**, 161–172 (2011).
34. Micchelli, C. A., Sudmeier, L., Perrimon, N., Tang, S. & Beehler-Evans, R. Identification of adult midgut precursors in *Drosophila*. *Gene Expr. Patterns* **11**, 12–21 (2011).
35. Takashima, S., Aghajanian, P., Younossi-Hartenstein, A. & Hartenstein, V. Origin and dynamic lineage characteristics of the developing *Drosophila* midgut stem cells. *Dev. Biol.* **416**, 347–360 (2016).
36. Knoblich, J. A., Jan, L. Y. & Jan, Y. N. Asymmetric segregation of Numb and Prospero during cell division. *Nature* **377**, 624–627 (1995).
37. Spana, E. P. & Doe, C. Q. The prospero transcription factor is asymmetrically localized to the cell cortex during neuroblast mitosis in *Drosophila*. *Development* **121**, 3187–3195 (1995).
38. Yin, C. & Xi, R. A phyllopod-mediated feedback loop promotes intestinal stem cell enteroendocrine commitment in *Drosophila*. *Stem Cell Rep.* https://doi.org/10.1016/j.stemcr.2017.11.014 (2017).
39. Novak, B. & Tyson, J. J. Design principles of biochemical oscillators. *Nat. Rev. Mol. Cell. Biol.* **9**, 981–991 (2008).
40. Clevers, H. The intestinal crypt, a prototype stem cell compartment. *Cell* **154**, 274–284 (2013).
41. Homem, C. C. & Knoblich, J. A. *Drosophila* neuroblasts: a model for stem cell biology. *Development* **139**, 4297–4310 (2012).
42. Choksi, S. P. et al. Prospero acts as a binary switch between self-renewal and differentiation in *Drosophila* neural stem cells. *Dev. Cell.* **11**, 775–789 (2006).
43. Olsson, A. et al. Single-cell analysis of mixed-lineage states leading to a binary cell fate choice. *Nature* **537**, 698–702 (2016).
44. Bechard, M. E. et al. Precommitment low-level Neurog3 expression defines a long-lived mitotic endocrine-biased progenitor pool that drives production of endocrine-committed cells. *Genes. Dev.* **30**, 1852–1865 (2016).
45. Kim, T. H. et al. Single-cell transcript profiles reveal multilineage priming in early progenitors derived from Lgr5$^+$ intestinal stem cells. *Cell. Rep.* **16**, 2053–2060 (2016).

Acknowledgements

The authors thank the members of the fly community, as identified in the Methods, for providing fly stocks and antibodies, the Bloomington *Drosophila* Stock Center, the Tsinghua Fly Center and the Developmental Studies Hybridoma Bank (DSHB) for reagents, and A. Spradling, J. Rajagopal and members of the Xi laboratory for critical reading, and J. Snyder for proofreading the manuscript. This work was supported by the National Key Research and Development Program of China (2017YFA0103602 to R.X), the National Basic Research Program of China (2014CB850002 and 2011CB812700 to R.X.) and the National Natural Science Foundation of China (31501105 to N.X.).

Author contributions

Conceptualization was provided by J.C. and R.X. Methodology was designed by J.C., N.X., C.W., P.H., Z.J., H.H., Z.Y., T.C., R.J. and R.X. Investigations were carried out by J.C., N.X., C.W., P.H., H.H. and R.X. Formal analysis was performed by J.C., N.X., C.W., P.H., Z.J., H.H. and R.X. The manuscript was written by J.C., H.H. and R.X.

Competing interests

The authors declare no competing financial interests.

Additional information

Supplementary information is available for this paper at https://doi.org/10.1038/s41556-017-0020-0.

Reprints and permissions information is available at www.nature.com/reprints.

Correspondence and requests for materials should be addressed to R.X.

Publisher's note: Springer Nature remains neutral with regard to jurisdictional claims in published maps and institutional affiliations.

Methods

Fly stocks. Female flies aged 4–7 days were selected for the experiments, unless otherwise noted. Animal care and use followed the institutional guidelines of the National Institute of Biological Sciences (NIBS), Beijing, and the authors affirm that the study is compliant with all relevant ethical regulations regarding animal research.

The following stocks were used in this study: UAS-sc-RNAi (BDSC, #26206)[46]; Esg-GAL4,UAS-GFP (gift from S. Hayashi); UAS-RedStinger (BDSC, #8547); Dl-GAL4 (gift from X. Zeng and S. Hou)[47]; GMR14C12-GAL4 (BDSC, #48607)[48]; UAS-RFP; UAS-Notch-RNAi (BDSC, #7078); UAS-Sc (BDSC, #26687); lea[2] (BDSC, #3102); m8-lacZ (BDSC, #26786); UAS-E(spl)m8-DamID (gift from F. Schweisguth)[49]; Df(3R) E(spl) b32.2 gro+[50]. The Scute-GFP knock-in line was generated by Cas9- mediated gene knock-in using a previously described protocol[51]. The GMR14C12-LacZ reporter line was generated by inserting the GMR14C12 DNA fragment into the multiple cloning site of C4PLZ vector, followed by P-element-mediated transformation. The m8-nlacZ reporter construct was generated by inserting the enhancer region of E(spl)m8 into the multiple cloning site of C4PLZ vector. The E1 or E2 site mutant m8-nlacZ reporter constructs were generated by site-directed mutagenesis, and in both cases, the E-box sequence 'CANNTG' was mutated to 'AANNGG'.

Immunostaining. Midgut samples were fixed and immunostained as previously described[52]. Briefly, midguts were dissected into cold Grace's media, and fixed in a mixture of 4% formaldehyde in PBS and *n*-heptane in an equal volume for 30 min. The lower phase of the mixture was then replaced with methanol, followed by vigorous shaking for 30 s. The samples were then washed once with 100% methanol for 5 min, followed by gradual rehydration in PBT (PBS with 0.1% Triton X-100). For staining with anti-GFP anybody, the fixation was done by incubating midguts with 4% formaldehyde in PBS for 30 min. Samples were then incubated in block (5% normal goat serum in PBT) for 1 h. Samples were stained with primary antibodies overnight at 4 °C, washed with PBT, and incubated with secondary antibodies for 2 h at room temperature or overnight at 4 °C. Samples were washed with PBT and mounted in 70% glycerol. The primary antibodies used in this study include mouse anti-Dl (Developmental Studies Hybridoma Bank, Iowa (DSHB), 1:100 dilution); mouse anti-Pros (DSHB, 1:300); rabbit anti-phospho-Histone H3 antibody (Cell Signaling Technology, 1:500); rabbit anti-GFP (Cell Signaling Technology, 1:200); rabbit polyclonal anti-lacZ antibody (Cappel, 1:6,000); rabbit anti-Pros (gift from Y.-N. Jan, 1:1,000); mouse anti-Allatostatin A (DSHB, 1:300); rabbit anti-tachykinin antibody (gift from D. Nassel, 1:300); rat anti-BrdU (Abcam, 1:200); and mouse anti-Cut (DSHB, 1:20). The secondary antibodies used in the study were goat anti-rabbit, anti-rat or anti-mouse IgGs-conjugated to Alexa (568 or Cy5) (Molecular Probes, 1:300). Images were acquired on a Zeiss LSM510 or LSM880 inverted confocal microscope. All images were assembled in Adobe Photoshop and Illustrator.

Binary GAL4/UAS system and mosaic analysis. The temporal and regional gene expression targeting (TARGET) system, which utilizes the binary GAL4/UAS system and a temperature-sensitive GAL80, was used for spatial and temporal control of transgene expression in fly midgut[53,54]. Crosses were carried out at 18 °C unless otherwise stated. Two- to three-day-old female progenies were then cultured at 29 °C with regular corn meal topped with fresh yeast paste. Flies were provided with new food every two days until analysis. For EE depletion and regeneration experiment, flies were transferred to 29 °C at L3 stage until eclosion. Female progenies with the desired genotype were cultured with regular corn meal with yeast paste for an additional 3 days. Half of the flies were dissected for EE depletion analysis, and the other half were shifted back to 18 °C and cultured with regular corn meal with yeast paste for another 3 days before analysis. Mosaic analysis with a repressible cell marker (MARCM) was used to generate GFP- or RFP-marked wild-type or mutant clones in the midgut epithelium[55]. Clones were induced by a 1 h heat-shock treatment in a 37 °C running water bath.

BrdU labelling. Flies were fed on standard corn meal supplemented with 2 mg ml^{-1} BrdU (Sigma-Aldrich) for 2 h. Half of the flies were immediately dissected and fixed for analysis (pulse BrdU), and another half were transferred to standard corn meal without BrdU supplement and cultured for an additional 4 days before analysis (BrdU chase). Midguts were dissected in Grace's medium and fixed in 4% formaldehyde in PBT for 30 min, followed by DNase I treatment for 15 min at 37 °C. The subsequent antibody staining steps were as described above.

Fluorescence-activated cell sorting (FACS) and RNA extraction. RNA-seq analysis of ISCs was performed according to a previously decribed method[56,57,58]. Briefly, 50 female guts were dissected into ice-cold diethyl pyrocarbonate (DEPC)-treated water-PBS, and incubated with 1 mg ml^{-1} Elastase (Sigma, cat. no. E0258) for 1 h at 25 °C, during which the sample was softly mixed every 15 min by pipetting and inverting four to six times. Dissociated samples were pelleted at 400*g* for 20 min at 25 °C, resuspended in 0.5 ml ice-cold DEPC-PBS, filtered with 40 µm filters (BD Falcon) and sorted using a FACS Aria II sorter (BD Biosciences). GFP$^+$ cells in the midgut of Dl-GAL4,UAS-GFP flies were sorted out, using w^{1118} midgut to set the fluorescence gate. For each of the three biological replicates, about 10,000 ISCs labelled with GFP were sorted, and RNA was harvested using the Arcturus PicoPure RNA isolation kit (Applied Biosystems) based on the manufacturer's protocol. The RNA was then amplified using an Arcturus RiboAmp HS PLUS RNA amplification kit (Applied Biosystems).

Single-end reads were mapped to the *Drosophila melanogaster* genome (Release 6) using STAR (v020201). Each sequencing experiment generated an average of 34.3 million raw reads, and 92% was uniquely mapped for each experiment. Gene expression was quantified, normalized and analysed as previously described[58].

RNA sequencing. In total, 1 µg RNA was used for cDNA construction for each sample. cDNA libraries were constructed using NEBNext DNA library prep master mix set (New England Biolabs, cat. no. E6040L) and NEBNext multiplex oligos (New England Biolabs, cat. nos. E7335S/E7500S). Libraries were qualified on an Agilent 2100 Bioanalyzer using an Agilent high-sensitivity DNA kit (Agilent Technologies, cat. no. 5067-1513), and then quantified using a Qubit dsDNA HS assay kit (Thermo Fisher Scientific, cat. no. Q32851) and an Illumina library quantification kit (Kapa Biosystems, cat. no. KK4824). All steps were performed according to the manufacturer's protocols. Sequencing was performed on an Illumina Hiseq-2500 sequencing system with 50 bp read length.

Bioinformatics analysis for RNA-seq data. Single-end reads were aligned against the *D. melanogaster* genome (Release 6) using STAR (v020201). Each sequencing experiment generated an average of 34.3 million raw reads, and 92% was uniquely mapped for each experiment. Gene expression was quantified by the number of reads that fall into the exons. The results were normalized to RPKM (reads per kilobase of exon model per million mapped reads) using Cufflinks (v2.2.1). Differentially expressed genes were identified by cuffdiff, and significantly differentially expressed genes were filtered with P values ≤ 0.05 and fold change of ≥ 2.

DamID. DamID was carried out according to a previously described method[59]. Briefly, the lines of Dl-GAL4, Gal80^{ts}, UAS-Dam, and Dl-GAL4, Gal80^{ts}, UAS-Dam-E(spl)m8, were used to harvest midgut two days after transgene expression at the adult stage. About 60 midguts were collected for gDNA isolation, then followed by DpnII and alkaline phosphatase treatment. The treated samples were digested with DpnI and ligated with adaptor for ligation-mediated polymerase chain reaction (LM-PCR). Following PCR, the amplified DNAs were treated with T7 exonuclease and purified for sequencing following fragmentation.

ChIP-seq reads were aligned using Bowtie (version 1.1.2) to build version BDGP6 of the *D. melanogaster* genome. MACS (version 1.4.1) was used to identify regions of ChIP-seq enrichment. The density of reads in each region was normalized to the total number of 10 million mapped reads. BigWig files were generated for visualization using the Homer package.

Statistics and reproducibility. Sample size was determined by previous experience with similar experimental designs. Typically, 10–30 flies were scored for each experiment, and all experiments were repeated at least three times unless otherwise indicated. For DamID experiments, one replicate was performed in which the relative enrichment peaks were determined by log(fold change) between Sc-Dam-expressed (experiment) and Dam-expressed (control) samples. Mitotic index was determined by counting the PH3$^+$ cells of whole midguts. The proportion of Sc$^+$ ISCs was determined as the number of Sc-GFP$^+$ cells in the total Dl$^+$ cells within a microscopic field, with the mean number, *n* number and standard error of the mean (s.e.m.) presented for each genotype. To analyse the first few rounds of cell division in *sc*-overexpressed ISCs, RedStinger$^+$ clones with three or fewer cells were taken for analysis. The number of cell divisions was deduced based on the total number of cells in each clone. The first cell division features one PH3$^+$ cell in a one-cell clone, the second division features one PH3$^+$ cell in a two-cell clone, and the third division features one PH3$^+$ cell in a three-cell clone. No other exclusion criteria were applied. No sample randomization or blinding was performed. Statistical analysis was performed using Graphpad Prism 6. All significance tests were carried out with unpaired two-tailed *t*-tests. *n* is as indicated in each figure. Significance values: NS, not significant ($P > 0.05$), *$P < 0.05$, **$P < 0.01$, ***$P < 0.001$, ****$P < 0.0001$.

Life Sciences Reporting Summary. Further information on experimental design is available in the Life Sciences Reporting Summary.

Data availability. DamID and RNA-seq data that support the findings of this study have been deposited in the Gene Expression Omnibus (GEO) under accession codes GSE102568 and GSE102569, respectively. Previously published ChIP-seq data that were reanalysed here are available under accession code GSE84283. Source data are provided in Supplementary Table 1. All other data supporting the findings of this study are available from the corresponding author upon reasonable request.

References

46. Ni, J. Q. et al. A genome-scale shRNA resource for transgenic RNAi in *Drosophila*. *Nat. Methods* **8**, 405–407 (2011).
47. Zeng, X., Chauhan, C. & Hou, S. X. Characterization of midgut stem cell- and enteroblast-specific Gal4 lines in *Drosophila*. *Genesis* **48**, 607–611 (2010).
48. Jenett, A. et al. A GAL4-driver line resource for *Drosophila* neurobiology. *Cell. Rep.* **2**, 991–1001 (2012).
49. Bivik, C. et al. Control of neural daughter cell proliferation by multi-level Notch/Su(H)/E(spl)-HLH signaling. *PLoS. Genet.* **12**, e1005984 (2016).
50. Schrons, H., Knust, E. & Campos-Ortega, J. A. The enhancer of split complex and adjacent genes in the 96F region of *Drosophila melanogaster* are required for segregation of neural and epidermal progenitor cells. *Genetics* **132**, 481–503 (1992).
51. Yu, Z. et al. Highly efficient genome modifications mediated by CRISPR/Cas9 in *Drosophila*. *Genetics* **195**, 289–291 (2013).
52. Lin, G., Xu, N. & Xi, R. Paracrine wingless signalling controls self-renewal of *Drosophila* intestinal stem cells. *Nature* **455**, 1119–1123 (2008).
53. Brand, A. H. & Perrimon, N. Targeted gene expression as a means of altering cell fates and generating dominant phenotypes. *Development* **118**, 401–415 (1993).
54. McGuire, S. E., Mao, Z. & Davis, R. L. Spatiotemporal gene expression targeting with the TARGET and gene-switch systems in *Drosophila*. *Sci. STKE* **2004**, pl6 (2004).
55. Lee, T. & Luo, L. Mosaic analysis with a repressible cell marker for studies of gene function in neuronal morphogenesis. *Neuron* **22**, 451–461 (1999).
56. Dutta, D., Xiang, J. & Edgar, B. A. RNA expression profiling from FACS-isolated cells of the *Drosophila* intestine. *Curr. Protoc. Stem Cell. Biol.* **27**, Unit 2F.2 (2013).
57. Chen, J., Xu, N., Huang, H., Cai, T. & Xi, R. A feedback amplification loop between stem cells and their progeny promotes tissue regeneration and tumorigenesis. *eLife* **5**, e14330 (2016).
58. Chen, J., Li, J., Huang, H. & Xi, R. Gene expression analysis of sorted cells by RNA-seq in *Drosophila* intestine. *Bio-Protoc.* **6**, e2079 (2016).
59. Gutierrez-Triana, J. A., Mateo, J. L., Ibberson, D., Ryu, S. & Wittbrodt, J. iDamIDseq and iDEAR: an improved method and computational pipeline to profile chromatin-binding proteins. *Development* **143**, 4272–4278 (2016).

nature research

Corresponding author(s): Rongwen Xi

☐ Initial submission ☐ Revised version ☒ Final submission

Life Sciences Reporting Summary

Nature Research wishes to improve the reproducibility of the work that we publish. This form is intended for publication with all accepted life science papers and provides structure for consistency and transparency in reporting. Every life science submission will use this form; some list items might not apply to an individual manuscript, but all fields must be completed for clarity.

For further information on the points included in this form, see Reporting Life Sciences Research. For further information on Nature Research policies, including our data availability policy, see Authors & Referees and the Editorial Policy Checklist.

Experimental design

1. Sample size

Describe how sample size was determined.

No statistics was used to predetermine sample size. Sample sizes were determined based on either our previous experiences or the published studies with similar experimental designs.

2. Data exclusions

Describe any data exclusions.

No data was excluded.

3. Replication

Describe whether the experimental findings were reliably reproduced.

All experiments were repeated at least three times unless otherwise indicated, and all attempts at replication were successful. For DamID experiments, one replicate was performed in which the relative enrichment peaks were determined by log (fold change) between Sc-Dam-expressed (experiment) and Dam-expressed (control) samples.

4. Randomization

Describe how samples/organisms/participants were allocated into experimental groups.

No randomization was applied.

5. Blinding

Describe whether the investigators were blinded to group allocation during data collection and/or analysis.

Investigators were not blinded to group allocation.

Note: all studies involving animals and/or human research participants must disclose whether blinding and randomization were used.

6. Statistical parameters

For all figures and tables that use statistical methods, confirm that the following items are present in relevant figure legends (or in the Methods section if additional space is needed).

n/a	Confirmed
☐	☒ The exact sample size (*n*) for each experimental group/condition, given as a discrete number and unit of measurement (animals, litters, cultures, etc.)
☐	☒ A description of how samples were collected, noting whether measurements were taken from distinct samples or whether the same sample was measured repeatedly
☐	☒ A statement indicating how many times each experiment was replicated
☐	☒ The statistical test(s) used and whether they are one- or two-sided (note: only common tests should be described solely by name; more complex techniques should be described in the Methods section)
☐	☒ A description of any assumptions or corrections, such as an adjustment for multiple comparisons
☐	☒ The test results (e.g. *P* values) given as exact values whenever possible and with confidence intervals noted
☐	☒ A clear description of statistics including central tendency (e.g. median, mean) and variation (e.g. standard deviation, interquartile range)
☐	☒ Clearly defined error bars

See the web collection on statistics for biologists for further resources and guidance.

Software

Policy information about availability of computer code

7. Software

Describe the software used to analyze the data in this study.	Prism 6, STAR (v020201), Cufflinks (v2.2.1), Bowtie (version 1.1.2), MACS (version 1.4.1)

For manuscripts utilizing custom algorithms or software that are central to the paper but not yet described in the published literature, software must be made available to editors and reviewers upon request. We strongly encourage code deposition in a community repository (e.g. GitHub). *Nature Methods* guidance for providing algorithms and software for publication provides further information on this topic.

Materials and reagents

Policy information about availability of materials

8. Materials availability

Indicate whether there are restrictions on availability of unique materials or if these materials are only available for distribution by a for-profit company.	All materials are readily available from authors or standard commercial sources

9. Antibodies

Describe the antibodies used and how they were validated for use in the system under study (i.e. assay and species).	mouse anti-Dl (DSHB, 1:100 dilution); mouse anti-Pros (DSHB, 1:300); mouse anti-phospho-Histone H3 antibody (Cell Signaling Technology, 1:500); rabbit anti-GFP (Cell Signaling Technology, 1:200); rabbit polyclonal anti-lacZ antibody (Cappel,1:6000); rabbit anti-Pros (gift from Yuh-Nung Jan, 1:1000); mouse anti-Allatostatin A (DSHB, 1:300); rabbit anti-Tachykinin antibody (a gift from Dick Nassel, 1:300); rat anti-BrdU (Abcam, 1:200); mouse anti-Cut (DSHB, 1:20). Secondary antibodies used in this study: goat anti-rabbit or anti-mouse IgGs-conjugated to Alexa (568 or Cy5) (Molecular Probes, 1:300). The commercial antibodies were validated based on the information on the manufacturers' instructions. The gift antibodies were validated based on the reported patterns.

10. Eukaryotic cell lines

a. State the source of each eukaryotic cell line used.	No cell lines were used in the manuscript.
b. Describe the method of cell line authentication used.	No cell lines were used in the manuscript.
c. Report whether the cell lines were tested for mycoplasma contamination.	No cell lines were used in the manuscript.
d. If any of the cell lines used are listed in the database of commonly misidentified cell lines maintained by ICLAC, provide a scientific rationale for their use.	No cell lines used in this study were found in the database of commonly misidentified cell lines that is maintained by ICLAC and NCBI Biosample.

Animals and human research participants

Policy information about studies involving animals; when reporting animal research, follow the ARRIVE guidelines

11. Description of research animals

Provide details on animals and/or animal-derived materials used in the study.	Female flies of 4-7 days old were selected for the experiments, unless otherwise noted. Duration of the experiment is dependent on each experimental design. The following fly lines were used in this study: UAS-sc-RNAi (BDSC, #26206); esg-GAL4,UAS-GFP (gift from Shigeo Hayashi); UAS-RedStinger (BDSC, #8547); Dl-GAL4 (gift from Xiankun Zeng and Steven Hou); GMR14C12-GAL4 (BDSC, #48607); UAS-RFP; UAS-Notch-RNAi (BDSC, #7078); UAS-Sc (BDSC, #26687); lea2 (BDSC, #3102); m8-lacZ (BDSC, #26786); UAS-E(spl)m8-DamID (gift from Francois Schweisguth); Df(3R) E(spl) b32.2 gro+. The Scute-GFP knock-in line was generated by Cas9-mediated gene knock-in using previously described protocol. The GMR14C12-LacZ reporter line was generated by inserting the GMR14C12 DNA fragment into the multiple cloning site of C4PLZ vector, followed by P-element-mediated transformation. The m8-nlacZ reporter construct was generated by inserting the enhancer region of E(spl)m8 into the multiple cloning site of C4PLZ vector. The E1 or E2 site mutant m8-nlacZ reporter constructs were generated by site-directed mutagenesis, and in both cases, the E-box sequence “CANNTG” was mutated to “AANNGG”.

Policy information about studies involving human research participants

12. Description of human research participants

Describe the covariate-relevant population characteristics of the human research participants.	This study did not involve human research participants.

nature research

Corresponding author(s): Rongwen Xi

☐ Initial submission ☐ Revised version ☒ Final submission

ChIP-seq Reporting Summary

Form fields will expand as needed. Please do not leave fields blank.

Data deposition

1. For all ChIP-seq data:

☒ a. Confirm that both raw and final processed data have been deposited in a public database such as GEO.

☒ b. Confirm that you have deposited or provided access to graph files (e.g. BED files) for the called peaks.

2. Provide all necessary reviewer access links. *The entry may remain private before publication.*	https://www.ncbi.nlm.nih.gov/geo/query/acc.cgi?acc=GSE102568.
3. Provide a list of all files available in the database submission.	Ctrl_Dam.fastq.gz;m8_Dam.fastq.gz;Ctrl_Dam.bw;m8_Dam.bw
4. If available, provide a link to an anonymized genome browser session (e.g. UCSC).	N.A.

Methodological details

5. Describe the experimental replicates.	No experimental replicates.
6. Describe the sequencing depth for each experiment.	10x coverage for Ctrl_Dam and 16x coverage for m8_Dam
7. Describe the antibodies used for the ChIP-seq experiments.	A DamID method was used, which does not need antibodies.
8. Describe the peak calling parameters.	Default parameters
9. Describe the methods used to ensure data quality.	The cutoff of peakcalling is pvalue<1e-5.
10. Describe the software used to collect and analyze the ChIP-seq data.	Bowtie(v1.1.2) and MACS(v1.4.2)